ARTICLE

Versatile microsphere attachment of GFP-labeled motors and other tagged proteins with preserved functionality

Michael Bugiel[1], Horatiu Fantana[2], Volker Bormuth[3], Anastasiya Trushko[4], Frederic Schiemann[1], Jonathon Howard[5], Erik Schäffer[1*], Anita Jannasch[1*]

[1]Centre for Plant Molecular Biology, University of Tübingen, Tübingen, Germany
[2]Max Planck Institute of Molecular Cell Biology and Genetics, Dresden, Germany
[3]Laboratoire Jean Perrin, Université Pierre et Marie Curie, Paris, France
[4]Biochemistry Department, University of Geneva, Geneva, Switzerland
[5]Yale School of Medicine, New Haven, Connecticut, USA

*Corresponding authors: Centre for Plant Molecular Biology, University of Tübingen, Auf der Morgenstelle 32, 72706 Tübingen, Germany, Erik.Schaeffer@uni-tuebingen.de or Anita.Jannasch@uni-tuebingen.de

Abstract Microspheres are often used as handles for protein purification or force spectroscopy. For example, optical tweezers apply forces on trapped particles to which motor proteins are attached. However, even though many attachment strategies exist, procedures are often limited to a particular biomolecule and prone to non-specific protein or surface attachment. Such interactions may lead to loss of protein functionality or microsphere clustering. Here, we describe a versatile coupling procedure for GFP-tagged proteins via a polyethylene glycol linker preserving the functionality of the coupled proteins. The procedure combines well-established protocols, is highly reproducible, reliable, and can be used for a large variety of proteins. The coupling is efficient and can be tuned to the desired microsphere-to-protein ratio. Moreover, microspheres hardly cluster or adhere to surfaces. Furthermore, the procedure can be adapted to different tags providing flexibility and a promising attachment strategy for any tagged protein.

Keywords: force spectroscopy, microsphere coupling, motor proteins, optical tweezers, PEGylation

INTRODUCTION

Coupling of molecular motors to surfaces such as microscope slides or microspheres is essential for the *in vitro* observation of motor protein movement. Especially for optical or magnetic tweezers experiments, coupling the protein of interest to microspheres is crucial for position and force measurements. Also key is to ensure that the protein remains functionally active after the coupling procedure. The first motor protein-coated surface protocols with kinesin-1 were based on a non-specific adsorption of kinesin on casein-coated glass slides or microspheres [1,2]. Kinesin-1, also called conventional kinesin, belongs to the super family of kinesins and uses ATP hydrolysis to translocate along microtubules. While the C-terminal tail domain of kinesin-1 naturally binds glass surfaces and the stalk is thought to be in a compact form not bound to the surface [3], casein helps to reduce non-specific interactions. Since truncated kinesin-1 or other kinesins have a different C-terminus, the non-specific, classic casein assay may not work. To achieve specific binding, microspheres are often coated with antibodies, which then bind to the complementary epitope of the motor protein. Those protocols

differ with respect to the coupling of the antibody to the microspheres (e.g. biotinylated anti-His bound to streptavidin-coated microspheres [4]; anti-flag bound to amino microspheres with glutaraldehyde and protein G [5]; anti-myc covalently [6] or anti-GFP unspecifically [7] bound to carboxylated polystyrene microspheres). Another option is to couple kinesins tagged with biotinylated DNA to streptavidin-coated microspheres [8,9]. Common problems of coupling protocols are microsphere clustering or adhesion to the sample surface. Furthermore, some coupling protocols are time-consuming and may require more attempts for successful coupling [10]. Here, we use a polyethylene glycol (PEG) linker to covalently bind the antibody to the microspheres (**Fig. 1**). The coupling uses the well-established NHS/EDC activation. In addition, to prevent microsphere aggregation, we simultaneously cover the microspheres with a dense monolayer of covalently-attached PEG molecules, which do not have any further reactive groups at the free end. PEGylation is widely used to efficiently passivate microspheres for *in vivo* [11-14] and *in vitro* [15-18] experiments and for different kinds of surfaces [19-21]. Also, there are other protocols that use PEG for functionalization [22,23]. Our combined procedure uses PEG both

as a blocking agent and linker. The procedure is reliable and suitable for the functional coupling of a large range of different kinesin families. Furthermore, our protocol is highly flexible and can be adapted for different PEG lengths, microsphere diameters, and antibodies, outperforming commercially available PEG-coated microspheres. Therefore, this procedure may be of interest for other assays and force spectroscopy techniques.

MATERIALS AND METHODS

Chemicals (source, catalog number)

If no source is given, chemicals were ordered from Sigma-Aldrich. ATP (Roche, 519979), boric acid (B6768), β-mercaptoethanol (M6250), BSA Alexa 594 conjugate (Invitrogen, A13101), casein (C7078), catalase (C9322), EDC (03449), EGTA (E4378), F-127 (P2443), glucose (G7528), glucose oxidase (G2133), magnesium chloride (VWR, 97061), MES (M3671), PIPES (P6757), potassium chloride (P9333), potassium hydroxide (P1767), sodium tetraborate (221732), sulfo-NHS (56485).

Microsphere preparation

Below, we describe a standard protocol for 590 nm-diameter polystyrene microspheres coated with a monofunctional, 2 kDa α-methoxy-ω-amino PEG (referred to as mPEG) and a heterobifunctional, 3 kDa α-amino-ω-carboxy PEG (referred to as hPEG) in a 9:1 ratio, bound to an anti-GFP antibody and kinesin-8. The protocol can be adapted for other microspheres, PEG lengths, antibodies, and proteins of interest.

Activation of carboxylated polystyrene microspheres

Carboxyl-functionalized polystyrene microspheres (25 µl) of the stock solution (Bangs Laboratories, order number PC03N/6487, diameter d = 590 nm, 10% solids, surface charge 28.5 µeq/g) are washed twice in 1000 µl MES buffer (50 mM, pH = 6.0, filtered). To wash the microspheres, the aliquot was centrifuged 3 min at 14,000 g and the supernatant was removed. Fresh buffer was added and the pellet was re-suspended. To ensure that the pellet is re-suspended well, we vortexed and sonicated the solution in a bath sonicater (Isonic CD-7810A) for 10 s each. Finally, the microsphere pellet was re-suspended in 250 µl MES buffer. (Note: The centrifuging step needs to be adapted for different microsphere sizes. For example, to avoid clustering, small microspheres [e.g. 320 nm diameter] were centrifuged 5 min at 5500 g.) Immediately before usage, 6.8 mg of EDC (molecular weight 191.7 g/mol) and 7.7 mg of sulfo-NHS (molecular weight 217.1 g/mol) were each dissolved in 100 µl MES buffer. The final EDC and sulfo-NHS concentrations were a hundred-fold higher than the total concentration of carboxyl groups on the microspheres (71 nmol). First, 20 µl of the sulfo-NHS solution, then 20 µl of the EDC solution were added to the washed microspheres and mixed well. The suspension was incubated for 15 min at 37°C and mixed at 600 rpm in a thermomixer. (Note: It is critical for the activation step that EDC and sulfo-NHS are freshly dissolved in MES buffer and added within 2 min to the microspheres. The protocol also worked for ten to thousand-fold higher concentrations of EDC and sulfo-NHS compared to the effective COOH concentration from the microspheres. EDC and sulfo-NHS were stored desiccated at -20°C and 4°C, respectively, and opened less than 12 times over half a year. The stock powders were warmed to room temperature before opening. Alternatively, one can weigh and aliquot EDC and sulfo-NHS under an argon atmosphere and store them for several months.) After incubation with EDC and sulfo-NHS, the activated microspheres were

washed twice in 500 µl MES. Finally, the microsphere pellet was re-suspended in 250 µl borate buffer (130 mM boric acid, 18 mM sodium tetraborate, pH = 8.5, filtered). EDC reacts with the carboxyl group and forms an amino-reactive O-acylisourea intermediate. This intermediate is susceptible to hydrolysis and short-lived in aqueous solutions. The addition of sulfo-NHS stabilizes the amino-reactive intermediate by converting it to an amino-reactive sulfo-NHS ester. The sulfo-NHS ester increases the efficiency of EDC-mediated coupling reactions [24]. (Note: The amino-reactive sulfo-NHS ester intermediate is still semi-stable. Washing and adding the PEGs should not take longer than 20 min.)

PEG coupling

7.8 mg of the heterobifunctional hPEG (NH$_2$-PEG-O-C$_3$H$_6$-COOH × HCl, 3 kDa, Rapp Polymere, Tübingen, Germany, order number 133000-20-32) were dissolved in 100 µl borate buffer. 9.4 mg of the monofunctional mPEG (CH$_3$O-PEG-NH$_2$, 2 kDa, Rapp Polymere, order number 122000-2) were dissolved in 20 µl borate buffer. 20 µl of the hPEG-borate solution were mixed with the 20 µl mPEG-borate solution. The mixed PEG-borate solution was then added to the activated microspheres in 250 µl borate buffer and mixed well (vortex for 5–10 s). (Note: The total amount of the functional group R-NH$_2$ should be ten to a hundred-fold higher than the amount of carboxyl groups on the microspheres.) The coupling reaction was allowed to proceed for 90 min at 37°C and mixed at 600 rpm in the thermomixer. To remove unreacted PEG after the incubation, coated microspheres were washed five times in 500 µl borate buffer by spinning them down and resuspending them. Finally, the microsphere pellet was resuspended in 250 µl MES buffer. The PEG-coated microspheres could be stored at 4°C for several months, before the antibody coating. (Note: The incubation can be extended to 150 min or overnight at 4°C.)

Protein adsorption on PEG-coated microspheres

Uncoated and PEG-coated microspheres without antibodies were incubated with BSA, that was fluorescently labeled with Alexa Fluor 594 in 10 mM acetate buffer (pH = 5.1, 2 h at room temperature). Following the incubation, the two microsphere populations were imaged separately and mixed in a ratio of 5:1 (coated: uncoated), respectively.

Antibody and Fab-fragment coupling

The microspheres were activated in a procedure identical to the first activation. (Note: We used the same amount of EDC and sulfo-NHS. In the second activation step, only 1 out of 10 PEGs should have a carboxyl group. All carboxyl groups on the microspheres should have either reacted or be inaccessible for further reactions. Therefore, the amount of EDC and sulfo-NHS should be a thousand-fold higher than the carboxyl group concentration of the activated hPEGs.) After the activation, the microspheres were washed and then re-suspended in 250 µl PBS (pH = 7.0, filtered) containing 10 µl anti-GFP antibody (monoclonal from mice, antibody facility of MPI-CBG, Dresden, Germany, 3 mg/ml in PBS), anti-β-tubulin (monoclonal from mice, Sigma-Aldrich, order number T7816—the same antibody that was used for microtubule immobilization), or anti-GFP Fab fragments (4 mg/ml, purified from the above-mentioned anti-GFP antibodies using the Fab generation kit from Thermo Scientific (order number 44885), antibody facility of MPI-CBG, Dresden, Germany), respectively. The suspension was incubated for 90 min at 37°C and mixed with 600 rpm in the thermomixer. Because of the large size of the antibodies (≈ 150 kDa) and Fab fragments (≈ 50 kDa), many amine groups are exposed on their surface. Therefore, we expect a random orientation of the covalently coupled antibodies or

Fab fragments. Finally, the microspheres were washed 3 times in PBS, re-suspended in 250 µl PBS and stored at 4°C. The microspheres were functional for up to three weeks.

Determination of microsphere concentration

The microsphere concentration was determined by comparison of the extinction spectrum of polystyrene-PEG-anti-GFP microspheres with the spectra of different dilutions of polystyrene microsphere solution from the stock. The extinction spectra were measured with a Nanodrop 1000 spectrophotometer.

Kinesin attachment to microspheres

The protocol is described for the yeast kinesin-8 Kip3 [25], but can be easily adopted for other kinesins. Before every experiment, Kip3 was incubated with the prepared microspheres. Kip3 (with a stock concentration of 168 nM) were diluted 10–10,000 × in motility solution (see below) corresponding to a kinesin per microsphere number of 6000–6. Diluted kinesin-8 (2 µl) was very gently mixed (slow pipetting with a low-protein-binding, 10-ml tip, 40 times up and down in 30 s) with 2 µl of 20 × diluted polystyrene-PEG-anti-GFP microspheres and incubated for 7 min at room temperature. The motility solution for Kip3 consisted of BRB80 (80 mM PIPES, 1 mM MgCl$_2$, 1 mM EGTA, 100 mM KOH,

pH = 6.9) with 112.5 mM KCl, 0.1 mg/ml casein, 1 mM ATP, and an anti-fade cocktail (0.5% β-mercaptoethanol, 20 mM glucose, 20 µg/ml glucose oxidase, 8 µg/ml catalase). (Note: Ungentle mixing–e.g. fast pipetting or air bubbles–leads to strongly reduced motility. The composition of the motility solution may vary for other kinesins, especially with respect to the salt concentration.)

Sample preparation and kinesin assay

Kinesin-coated microsphere assays were performed in a flow cell. Flow cells were constructed as described in [25]. Microtubules were immobilized on a hydrophobic sample surface by anti-tubulin antibodies. The rest of the surface was blocked by Pluronic F-127. Kinesin-coated microspheres were flushed into the flow cell. Using the optical tweezers, a trapped microsphere was placed on top of a microtubule to await kinesin-initiated motility.

Optical tweezers and TIRF setup

The measurements were performed in a single-beam optical tweezers. The setup and calibration procedures are described in detail in [26-28]. Fluorescence measurements were performed in a TIRF microscope, described in [29].
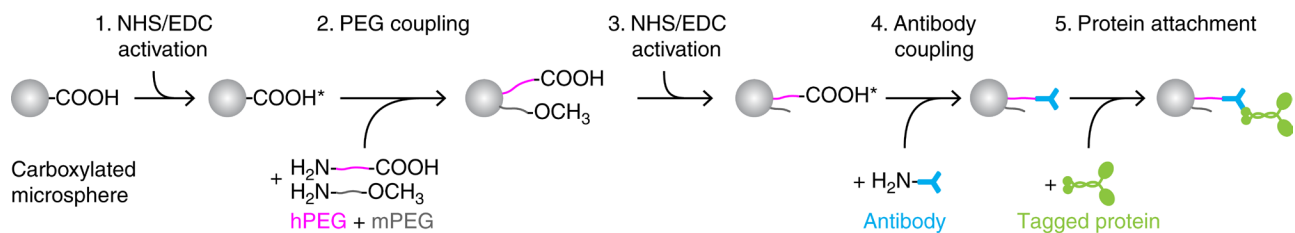

Figure 1. Schematic of the PEG-mediated, protein-attachment procedure. The monofunctional mPEG and heterobifunctional hPEG (ratio = 9:1) are covalently bound to the activated (indicated by an asterisk), carboxylated microsphere. The mPEG forms a non-reactive polymer brush on the microsphere's surface suppressing non-specific interactions. The antibodies (e.g. anti-GFP) are covalently bound in a random orientation to the activated carboxyl groups of the hPEG. Finally, the eGFP-tagged protein binds to the anti-GFP. Not drawn to scale.

Table 1. Speeds of free motors and motors, attached to microspheres.

Protein	ATP concentration (mM)	Free motors ν ± SEM (nm/s)	Motors, attached to microspheres ν ± SEM (nm/s)
rkin430	0.1	603 ± 26 (N = 98)	546 ± 84 (N = 10)
Kip3	1	41.0 ± 0.6 (N = 167)	40.0 ± 1.6 (N = 52)
Kif18A	1	181 ± 4 (N = 9)	162 ± 10 (N = 6)

ν, mean speed; SEM, standard errors of the means; N, number of data points. The speeds of motors coupled to microspheres were not statistically significant different to speeds of free motors (two-tailed t-test with the level of significance set to a probability P > 0.05).

RESULTS AND DISCUSSION

PEG-coated microspheres showed specific and no unspecific binding

Using our protocol, we covalently coupled a GFP antibody to carboxylated microspheres via a small fraction of a heterobifunctional PEG linker (hPEG) surrounded by many monofunctional PEG molecules

(mPEG), which have no additional molecules bound to their ends (Materials and Methods, **Fig. 1**). The shorter mPEG forms a polymeric brush that suppresses unspecific binding. To test for unspecific binding, we incubated fluorescent BSA with PEG-coated and uncoated microspheres. We imaged both types of microspheres using bright-field and fluorescence microscopy. Only for the uncoated microspheres, we measured a strong fluorescence signal. For a direct comparison of the fluorescence signals, we also imaged a mixture of these microspheres under identical illumination and imaging conditions (**Figs. 2A** and **2B**). While the uncoated microspheres were fluorescent, the PEG-coated microspheres displayed only a small level of remnant fluorescence (< 2% based on the integrated intensity of microspheres from the two populations). The low amount of fluorescence indicates that the PEG coupling procedure had profoundly reduced the non-specific protein binding capacity of the microsphere surface. Subsequently, we tested for specific binding using different GFP-labeled motor proteins: truncated rat kinesin-1 (his$_6$-rkin430-eGFP), budding yeast kinesin-8 (his$_6$-Kip3-eGFP, his$_6$-eGFP-Kip3, Kip3-his$_6$-eGFP), human kinesin-8 (his$_6$-Kif18A-eGFP), and orphan (ungrouped) kinesin Kip2 (his$_6$-Kip2-GFP, his$_6$-GFP-Kip2). Furthermore, we coupled the microspheres to the microtubule-polymerizing protein XMAP215-GFP-his$_7$ as described in [30]. For all proteins, we observed functional activity via microtubule interactions. All measurements using these microspheres (see below)

were reproducible and stable, showing that our coupling protocol is flexible and can be applied to many kinds of proteins.

Molecular motors attached to microspheres were functional

To test if the coupling procedure affected the functionality of the kinesin motors, we compared the average speed of free motors to the speed of motors attached to microspheres. The speeds of free motors were measured by tracking single fluorescently labeled motor molecules moving along immobilized microtubules in a TIRF microscope. The

speeds of the motor-attached-microspheres were determined by tracking them in DIC time-lapse images (**Fig. 2C**). The results for three different kinesins (rkin430, Kip3 and Kif18A) are shown in **Table 1**. Within error margins, the speeds were consistent with the TIRF measurements and literature values [29,31,32], confirming the functionality of the motor when attached to a microsphere. We also bound yeast kinesin-8 to microspheres following the classic casein protocol [1,2], but observed no motility. This lack of motility was our initial motivation to develop an efficient protocol for functional-protein attachment.
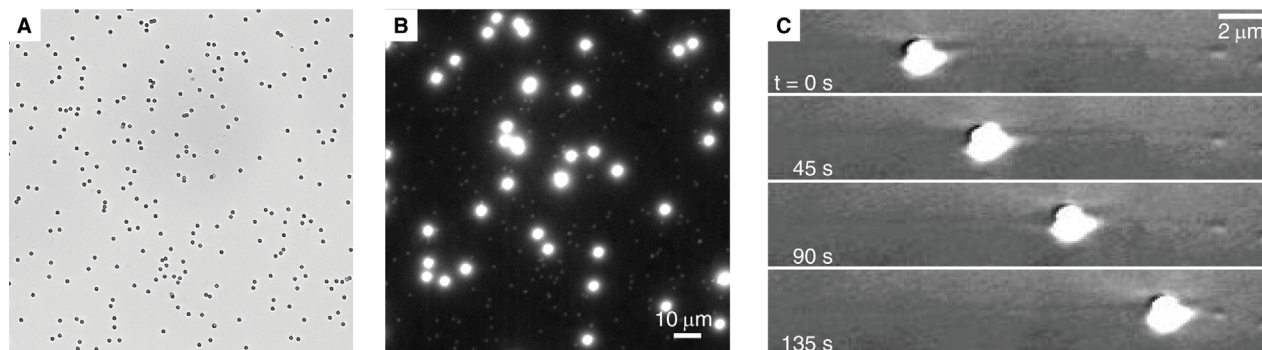

Figure 2. Prevention of unspecific and confirmation of specific binding. A and **B.** Bright-field (A) and fluorescence image (B)(same field of view), showing the two populations PEG-coated (no antibody) and uncoated microspheres, mixed in a ratio of 5:1 (PEG-coated:uncoated) after incubation with fluorescent BSA. In (B), the dynamic range of the image was adjusted to show the dim population of PEG-coated microspheres, thereby saturating the intensity signal of the uncoated microspheres. **C.** Differential interference contrast (DIC) images of a his_6-Kip3-eGFP-functionalized microsphere moving along a microtubule
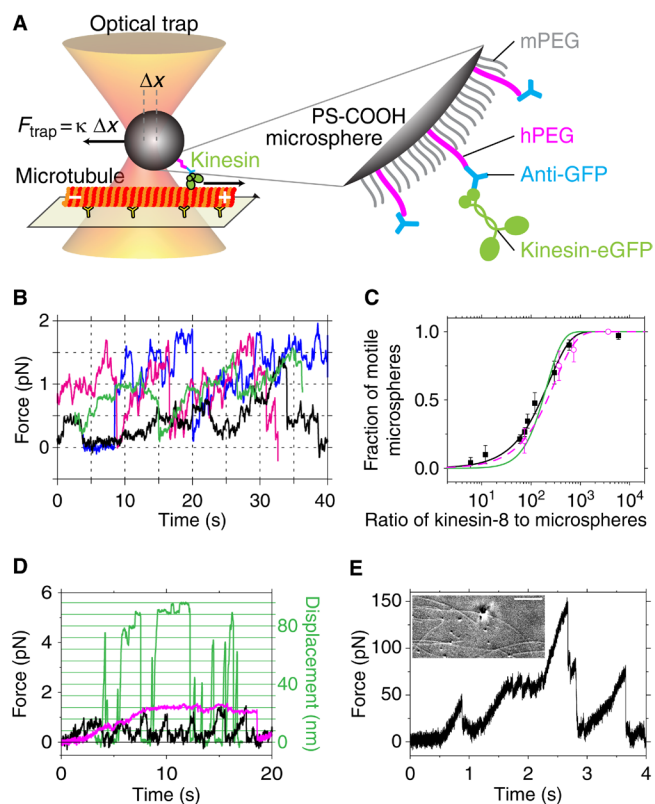

Figure 3. Motility measurements with preserved functionality. A. Schematic of an optical tweezers single-molecule experiment with kinesins. **B.** Stall-force measurements of single his_6-Kip3-eGFP, using microspheres with anti-GFP and without hPEG (magenta), with antigen-binding fragments

of anti-GFP (black), with antigen-binding fragments and without hPEG (blue), and with NeutrAvidin and biotinylated anti-GFP antibody (green). Sampling rate: 4 kHz, median filtered to 8 Hz. **C.** Fraction of motile microspheres P as a function of kinesin-8–motors–to–microsphere ratio n. Plotted are data from 590-nm diameter polystyrene microspheres, coated with 2 kDa mPEG and 3 kDa hPEG (filled black square: mPEG:hPEG = 9:1, open magenta circle: with anti-GFP antigen-binding fragment (Fab), mPEG:hPEG = 1:1). The data points (number of tested microspheres each ≥21) are fitted with $P_{\geq 1}(n) = 1 - e^{-\Gamma n}$ for at least one functional molecule per microsphere (black line for the anti-GFP microspheres, magenta dashed line for Fab) and $P_{\geq 2}(n) = 1 - e^{-\Gamma n} - \Gamma n e^{-\Gamma n}$ for two or more molecules per microsphere (green line for anti-GFP microspheres) [2]. **D.** Stall-force measurements of single his_6-Kip3-eGFP (magenta), his_6-Kif18A-eGFP (black) and his_6-rkin430-eGFP (green) motor proteins. Sampling rate: 10 kHz, box car filtered to 50 Hz (except rkin430: 4 kHz, median filtered to 8 Hz). Microsphere displacement for rkin430, only (right axis, green scale and grid). **E.** Forces on an anti-tubulin-coated microsphere, bound to a microtubule. Forces were measured in an optical trap and applied by moving the sample with constant speed parallel to the microtubule. Inset: DIC image of a microsphere, coated with anti-tubulin antibodies that was bound specifically to a microtubule. Scale bar is 5 μm.

The protocol was efficient

The protocol was fast and led to highly reproducible results. For example, for the standard preparation with 590-nm diameter microspheres coated with 2 kDa mPEG and 3 kDa hPEG in a ratio 9:1, 36 out of 39 microsphere preparations were successful. We defined an experiment as successful if at least 18 out of 20 microspheres showed motility at saturating ATP (1 mM) and motor concentrations. The preparation of

the microspheres took about 5 hr. The microspheres with the antibody could then be used for at least 3 weeks. Furthermore in one experiment, we shock-froze the microspheres with bound XMAP215 (no single-molecule conditions) and kept them at -80°C. After 6 months, the microspheres still showed functionality [30].

Table 2. List of different microsphere sizes and molecular weights of used hPEG and mPEG.

Microsphere diameter (nm)	hPEG (kDa)	mPEG (kDa)	Motility[1]	Single microspheres /clusters[2]
820	10	5	13/13	19/1
820	1	2	10/10	18/2
590	10	5	20/20	18/2
590	5	2	17/17	18/2
590[3]	**3**	**2**	**37/37**	**18/2**
590	1	2	25/25	19/1
590	2	0.75	8/19	4/16
590	-	2	10/10	19/1
510	10	5	12/12	18/2
510	5	2	7/7	18/2
320	10	5	6/6	16/4
320	5	2	9/9	15/5
320	3	2	7/7	15/5
320	1	2	11/11	14/6
320	2	0.75	1/10	2/18
320	1	0.5	1/11	3/17

[1]The column "Motility" describes the fraction of motile microspheres. [2]The column "Single microspheres/clusters" provides the number of single microspheres and microsphere clusters of any size. The mPEG:hPEG ratio was 9:1 for all preparations with both PEGs. The tests were done at saturating kinesin (>1000 kinesins/microsphere) and ATP concentrations (1 mM). [3]The bold row indicates the standard preparation, described in the Materials and Methods section.
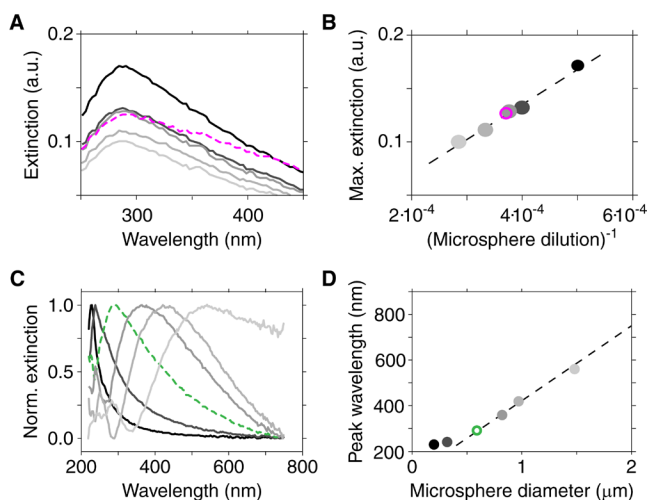
Figure 4. Measurement of microsphere concentration. A. Extinction spectra for different stock microsphere (590 nm PS-COOH) dilutions (2000, 2500, 2700, 3000, 3500: lines from black to light gray) and one batch of diluted anti-GFP-PEG-coated PS microspheres (magenta dashed line, 1000). **B.** Maximum extinction for 590 nm-diameter microspheres at 290 nm as function of (microsphere dilutions)$^{-1}$ (colors correspond to (A) with a linear fit (black dashed line). The peak height was inversely proportional to the microsphere dilution. **C.** Normalized extinction spectra for different microsphere diameters (200 nm, 320 nm, 820 nm, 970 nm, 1480 nm: lines from black to light gray; 590 nm: green dashed line). **D.** Peak wavelength of the extinction spectra as function of the microsphere diameter with a linear fit (dashed line) for diameters ≥ 590 nm. Symbol colors are given in (C).

Preparations with different microsphere sizes and PEG lengths showed motility and no clustering

The spatial signal-to-noise ratio of a trapped microsphere in an optical tweezers (**Fig. 3A**) and thus the accessible spatial resolution is, among other factors, influenced by the linker stiffness and the probe size, i.e. the microsphere diameter [33]. A small microsphere and a short linker are desirable for highest resolution. However, if the linker is too short or the protein is directly coupled to a surface, the functionality of the proteins may be influenced. To test under which conditions we had preserved protein functionality, we varied the microsphere diameter and PEG length (defined by their molecular weights). We tested different combinations in a kinesin-8 motility assay. **Table 2** shows that our protocol worked for a broad range of PEG lengths and microsphere sizes. For our experiments, not only the motility (fraction of motile microspheres) but also the amount of microsphere clustering was important. To this end, in a given field of view, we counted the ratio of single microspheres relative to clusters of any size. We found that a minimal length of mPEG with a molecular weight larger than 0.75 kDa was necessary to avoid clustering and ensure motility. Using our standard microspheres, we could reduce the amount of clustering

compared to e.g. a NeutrAvidin-biotin linkage [10] by a factor of two. The contour lengths of our two standard 3 kDa and 2 kDa PEGs are 23.4 nm and 15.7 nm, respectively [24]. Previous measurements with these microspheres revealed that the hPEG was stretched to its contour length under a load of about 1 pN (Fig. S10B in [34]). For the yeast kinesin-8 at this load, the overall length of the hPEG-antibody-kinesin tether was about 60 nm. At a reduced load of 0.5 pN, this length was about 34 nm. For the truncated rat kinesin-1 at 0.5 pN, the tether was about 52 nm long. To reduce the linker length as much as possible, we tested 590 nm microspheres without any hPEG. The antibodies, together with mPEG, were coupled directly to the carboxyl groups on the microsphere surface requiring only one activation step. In a yeast kinesin-8 assay, we found that an antibody-to-mPEG ratio of about 1:23,000 yielded functional microspheres (**Fig. 3B**). For this ratio, we also observed a low number of clusters. Using less mPEG led to increased cluster formation. Clustering may be caused by multiple amine groups on the antibodies that could lead to cross-linking of several microspheres if the repulsive effect of the PEG brush is compromised. The fraction of motile microspheres and, thus, single-molecule conditions could be further tuned by varying the kinesin-to-microsphere number (see below). For the direct-antibody-coupled microspheres, this fraction was generally smaller at comparable kinesin concentrations than for microspheres with the spacer hPEG. The smaller fraction indicates that using hPEG as a linker between the kinesin and the microsphere helped to preserve the kinesin's functionality.

The final microsphere concentration was measured with a spectrophotometer

To determine the absolute motor-to-microsphere ratio, we measured the microsphere concentration. Because of liquid transfers and surface adsorption, we usually lost an unknown number of microspheres during the preparation. Therefore, we determined the final microsphere concentration by measuring the extinction of visible and near-ultraviolet light (220-750 nm) by the functionalized microspheres at a specific wavelength (**Fig. 4A**). As a reference, we measured the extinction at the same wavelength by uncoated microspheres of known concentration. Extinction includes both absorption and scattering of the light by the microspheres. The extinction peak height scaled linearly with the microsphere concentration (**Fig. 4B**) and was used as a calibration. According to our measurements, a loss of 50-60% of the microspheres was typical during a preparation. The wavelength of the extinction peak depended on the microsphere diameter, which is consistent with the literature [35]. **Figure 4C** and **4D** show extinction spectra and peak wavelengths for different microsphere diameters. The peak wavelength increased with increasing diameters and could be used to determine the microsphere size.

Single-molecule measurements with kinesins were feasible

Single-molecule conditions, i.e. the interaction of only one motor protein per microsphere with the microtubule, can be reached by controlling the density of motors on the microsphere surface via the fraction of microspheres that show motility. A statistical analysis of the interaction probability of motor-coated microspheres with immobilized microtubules [2] shows that this fraction is a function of the motor-to-microsphere ratio and follows Poisson statistics. Single-molecule conditions with at least 95% confidence are achieved for a low motor-to-microsphere ratio if only 1 out of 3 microspheres shows motility. In **Figure 3C**, the fraction of motile microspheres decreased with lower motor-to-microsphere

ratios consistent with the expected Poisson statistics. Therefore, using our protocol, single-molecule conditions can be achieved. In addition to the speeds in **Table 1**, we measured the maximum forces that Kip3, Kif18A, and Kinesin-1 can generate (**Fig. 3D**). All measurements were performed under single-molecule conditions. Kip3 stalled at ≈1.2 pN, Kif18A at ≈1 pN, and Kinesin-1 at 5-6 pN. The values for Kinesin-1 and Kip3 are consistent with previously reported values [31,36] and support the notion that the functionality of the coupled proteins is preserved. We expect that the anti-GFP–kinesin linkage can sustain forces of at least 10 pN for several seconds [34].

Preparations with different mPEG-to-hPEG ratios produced functional motor-coupled microspheres

To reach single molecule conditions, either the motor-to-microsphere ratio or the density of antibodies on the microspheres can be reduced. To achieve the latter, we varied the mPEG (2 kDa)-to-hPEG (3 kDa) ratio from 9:1 to 9,999:1 in the preparation. Subsequently, we tested the microspheres with yeast kinesin-8. We observed motility at ratios of 9:1 (ratio of motile to total number of tested microspheres, 34/35 = 97%), 99:1 (9/20 = 45%) and 999:1 (2/17 = 12%) at saturating kinesin concentrations during the antibody coupling step. At 9,999:1 we had no motility (0/20 = 0%). Thus, with a 999:1 ratio, single-molecule conditions were given. These experiments show that our protocol is working with various mPEG-to-hPEG ratios requiring a minimal hPEG fraction. The advantage of a reduced antibody concentration is that irrespective of the motor concentration used for coupling, always single-molecule conditions are achieved.

Single kinesin steps were resolved

For single-molecule trajectories and subsequent modeling of kinesin-experiments, it is desirable to resolve the 8 nm steps that are typical for kinesins [37]. We tested our motor-coupled microspheres for this feature. We could observe clear steps for truncated rat kinesin-1 (**Fig. 3D**, green scale and grid). Because of the linker's non-linear elasticity, steps are more difficult to resolve at lower forces. We were also able to resolve 8 nm steps at forces as low as 1 pN for the yeast kinesin-8 Kip3 [25]. Thus, at these forces and using our standard hPEG molecular weight of 3 kDa, the linker was sufficiently stiff to provide high-resolution, single-molecule trajectories. Because we observed motility in the absence and for shorter 1 kDa hPEG linkers, we expect that a higher spatial resolution with the same bandwidth is feasible.

Preparations with antigen-binding fragments, NeutrAvidin, and anti-tubulin produced functional microspheres

To test the versatility of our protocol, we coupled proteins via different binding proteins and tags to the microspheres. Because antibodies (like anti-GFP) have more than one antigen binding site, one or more motor proteins could bind to the same antibody (disregarding steric constraints) potentially compromising single-molecule conditions. As shown above, using the protocol with anti-GFP, we were able to achieve single-molecule conditions (**Fig. 3C**). Thus, binding of two motors to a single antibody appears to be unlikely. Nevertheless, to rule out the possibility completely, we tested the protocol with purified antigen-binding fragments (Fab) of anti-GFP antibodies that have only one GFP-binding site per molecule (Materials and Methods). Such microspheres showed motility with yeast kinesin-8, followed Poisson statistics, and could be tuned to single-molecule conditions (**Fig. 3B** and **3C**). The fraction of motile Fab-based microspheres for a 1:1 mPEG:hPEG ratio was within error bars comparable to the antibody-coupled microspheres.

POL SCIENTIFIC

For Fab-based microspheres with the same mPEG:hPEG ratio as the standard anti-GFP preparation, the fraction of motile microspheres was generally smaller (data not shown). This smaller fraction may originate from carboxyl groups binding to the antigen binding site of the Fab fragment blocking motor coupling. In case of an antibody, another free binding site would still be left increasing the total number of motor binding sites per microsphere. Additionally, we tested microspheres with antigen-binding fragments directly bound to the microspheres (i.e. without hPEG) together with 2 kDa mPEG in a 1:2300 ratio (higher than the previously used ratio for the direct antibody coupling). These microspheres were also functional (**Fig. 3B**). Besides the coupling of GFP-tagged proteins to the corresponding antibodies or antigen-binding fragments, we tested other tags. We bound NeutrAvidin together with mPEG to the microsphere surface in a 1:10,000 ratio. Less mPEG led to cluster formation. These microspheres were subsequently incubated with biotinylated anti-GFP antibodies and tested successfully with yeast kinesin-8 (**Fig. 3B**). The NeutrAvidin-coated microspheres could also be bound to biotinylated giant unilamellar vesicles for membrane-tether-pulling experiments [38]. Furthermore, we coupled anti-tubulin instead of anti-GFP to microspheres (Materials and Methods). These microspheres were attached to microtubules. Using optical tweezers, we observed a strong, specific microsphere-microtubule interaction sustaining forces >100 pN (**Fig. 3E**, **Movie S1**). Thus, our microsphere preparation allows for specific interactions using various tags while preserving the functionality of the coupled proteins. In addition to *in vitro* measurements, the microspheres can also be used for *in vivo* experiments [39]. PEG-coated microspheres could be introduced into living cells. In such cells, the mPEG brush blocked the microsphere surface from non-specific interactions, whereas the antibody at the hPEG allowed for specific binding. Because the number of specific binding sites can be varied, single-molecule *in vivo* measurements may be possible with this microsphere design.

Acknowledgments

References

1. Howard J, Hudspeth AJ, Vale RD (1989) Movement of microtubules by single kinesin molecules. Nature 342: 154-158. doi: 10.1038/342154a0. PMID: 2530455

2. Block SM, Goldstein LS, Schnapp BJ (1990) Bead movement by single kinesin molecules studied with optical tweezers. Nature 348: 348-352. doi: 10.1038/348348a0. PMID: 2174512

3. Kerssemakers JWJ, Howard J, Hess H, Diez S (2006) The distance that kinesin-1 holds its cargo from the microtubule surface measured by fluorescence interference contrast microscopy. Proc Natl Acad Sci USA 103: 15812-15817. doi: 10.1073/pnas.0510400103. PMID: 17035506

4. Asbury CL, Fehr AN, Block SM (2003) Kinesin moves by an asymmetric hand-over-hand mechanism. Science 302: 2130-2134. doi: 10.1126/science.1092985. PMID: 14657506

5. Brunnbauer M, Dombi R, Ho TH, Schliwa M, Rief M, et al. (2012) Torque Generation of Kinesin Motors Is Governed by the Stability of the Neck Domain. Mol Cell 46: 147-158. doi: 10.1016/j.molcel.2012.04.005. PMID: 22541555

6. Oguchi Y, Uchimura S, Ohki T, Mikhailenko SV, Ishiwata S (2011) The bidirectional depolymerizer MCAK generates force by disassembling both microtubule ends. Nat Cell Biol 13: 846-852. doi: 10.1038/ncb2256. PMID: 21602793

7. Spudich JA, Rice SE, Rock SR, Purcell TJ, Warrick HM (2011) Attachment of Anti-GFP Antibodies to Microspheres for Optical Trapping Experiments. Cold Spring Harb Protoc. Cold Spring Harb Protoc 11: 1370-1. doi: 10.1101/pdb.prot066670. PMID: 22046049

8. Guydosh NR, Block SM (2009) Direct observation of the binding state of the kinesin head to the microtubule. Nature 461: 125-128. doi: 10.1038/nature08259. PMID: 19693012

9. Jamison DK, Driver JW, Rogers AR, Constantinou PE, Diehl MR (2010) Two kinesins transport cargo primarily via the action of one motor: implications for intracellular transport. Biophys J 99: 2967-2977. doi: 10.1016/j.bpj.2010.08.025. PMID: 21044594

10. Bormuth V, Zörgibel F, Schäffer E, Howard J (2011) Single Molecule Enzymology. Vol. 778 of Methods in Molecular Biology. Humana Press; 2011

11. Gbadamosi JK, Hunter AC, Moghimi SM (2002) PEGylation of microspheres generates a heterogeneous population of particles with differential surface characteristics and biological performance. FEBS letters 532: 338-344. PMID: 12482589

12. Sinha V, Aggarwal A, Trehan A (2004) Biodegradable PEGylated microspheres and nanospheres. Am J Drug Deliv 2(3): 157-171.

13. Madani F, Bessodes M, Lakrouf A, Vauthier C, Scherman D, et al. (2006) PEGylation of microspheres for therapeutic embolization: preparation, characterization and biological performance evaluation. Biomaterials 28: 1198-1208. doi: 10.1016/j.biomaterials.2006.10.017. PMID: 17113637

14. Byeon HJ, Kim I, Choi JS, Lee ES, Shin BS, et al. (2015) PEGylated apoptotic protein-loaded PLGA microspheres for cancer therapy. Int J Nanomedicine 10: 739-748. doi: 10.2147/IJN.S75821. PMID: 25632232

15. Caldwell KD (1997) Surface modifications with adsorbed poly(ethylene oxide)-based block copolymers. Physical characteristics and biological use. ACS Symposium Series 680: 400-419.

16. Valentine MT, Perlman ZE, Gardel ML, Shin JH, Matsudaira P, et al. (2004) Colloid Surface Chemistry Critically Affects Multiple Particle Tracking Measurements of Biomaterials. Biophys J 86: 4004-4014. doi: 10.1529/biophysj.103.037812. PMID: 15189896

17. Upadhyayula S, Quinata T, Bishop S, Gupta S, Johnson NR, et al. (2012) Coatings of Polyethylene Glycol for Suppressing Adhesion between Solid Microspheres and Flat Surfaces. Langmuir 28: 5059-5069. doi: 10.1021/la300545v. PMID: 22364506

18. Lu HB, Campbell CT, Castner DG (2000) Attachment of Functionalized Poly(ethylene glycol) Films to Gold Surfaces. Langmuir 16: 1711-1718. doi: 10.1021/la990221m.

19. Prime K, Whitesides G (1997) Self-assembled organic monolayers: model systems for studying adsorption of proteins at surfaces. Science 252: 1164-1167. PMID: 2031186

20. Kanaras AG, Kamounah FS, Schaumburg K, Kiely CJ, Brust M (2002) Thioalkylated tetraethylene glycol: a new ligand for water soluble monolayer protected gold clusters. Chem Commun 20: 2294-2295. PMID: 12430408

21. Uyeda HT, Medintz IL, Jaiswal JK, Simon SM, Mattoussi H (2005) Synthesis of Compact Multidentate Ligands to Prepare Stable Hydrophilic Quantum Dot Fluorophores. J Am Chem Soc 127: 3870-3878. doi: 10.1021/ja044031w. PMID: 15771523

22. Müller M, Vörös J, Csúcs G, Walter E, Danuser G, et al. (2003) Surface modification of PLGA microspheres. J Biomed Mater Res A 66: 55-61. doi: 10.1002/jbm.a.10502. PMID: 12833431

23. Breed DR, Thibault R, Xie F, Wang Q, Hawker CJ, et al. (2009) Functionalization of Polymer Microspheres Using Click Chemistry. Langmuir 25: 4370-4376. doi: 10.1021/la801880u. PMID: 19260650

24. Hermanson GT (2008) Bioconjugate techniques. Academic Press pp. 215-223.

25. Jannasch A, Bormuth V, Storch M, Howard J, Schäffer E (2013) Kinesin-8 Is a Low-Force Motor Protein with a Weakly Bound Slip State. Biophys J 104: 2456-2464. doi: 10.1016/j.bpj.2013.02.040. PMID: 23746518

26. Bormuth V, Howard J, Schäffer E (2007) LED illumination for video-enhanced DIC imaging of single microtubules. J Microsc 226: 1-5. doi: 10.1111/j.1365-2818.2007.01756.x. PMID: 17381703

27. Schäffer E, Nørrelykke SF, Howard J (2007) Surface forces and drag coefficients of microspheres near a plane surface measured with optical tweezers. Langmuir 23: 3654-3665. doi: 10.1021/la0622368. PMID: 17326669

28. Tolic-Nørrelykke SF, Schäffer E, Howard J, Pavone FS, Jülicher F, et al. (2006) Calibration of optical tweezers with positional detection in the back focal plane. Rev Sci Instrum 77: doi: 10.1063/1.2356852.

29. Varga V, Helenius J, Tanaka K, Hyman AA, Tanaka TU, et al. (2006) Yeast kinesin-8 depolymerizes microtubules in a length-dependent manner. Nat Cell Biol 8: 957-962. doi: 10.1038/ncb1462. PMID: 16906145

30. Trushko A, Schäffer E, Howard J (2013) The growth speed of microtubules with XMAP215-coated beads coupled to their ends is increased by tensile force. Proc Natl Acad Sci U S A 110: 14670-14675. doi: 10.1073/pnas.1218053110. PMID: 23964126

31. Svoboda K, Block SM (1994) Force and velocity measured for single kinesin molecules. Cell 77: 773-784. PMID: 8205624

32. Mayr MI, Storch M, Howard J, Mayer TU (2011) A non-motor microtubule binding site is essential for the high processivity and mitotic function of kinesin-8 Kif18A. PLoS One 6: doi: 10.1371/journal.pone.0027471. PMID: 22102900

33. Gittes F, Schmidt CF (1998) Signals and noise in micromechanical measurements. Methods Cell Biol 55: 129-156. PMID: 9352515

34. Bugiel M, Böhl E, Schäffer E (2015) The kinesin-8, Kip3, switches microtubule protofilaments in a sideward random walk asymmetrically biased by force. Biophys J 108: 2019-2027. doi: 10.1016/j.bpj.2015.03.022. PMID: 25902441

35. Bohren CF, Huffmann DR (1983) Absorption and scattering of light by small particles. Wiley-Interscience. pp. 317-318.

36. Bormuth V, Varga V, Howard J, Schäffer E (2009) Protein Friction Limits Diffusive and Directed movements of Kinesin Motors on Microtubules. Science 325: 870-873. doi: 10.1126/science.1174923. PMID: 19679813

37. Svoboda K, Schmidt CF, Schnapp BJ, Block SM (1993) Direct observation of kinesin stepping by optical trapping interferometry. Nature 365: 721-727. doi: 10.1038/365721a0. PMID: 8413650

38. Hermsdorf G (2013) Single-molecule fluorescence combined with optical tweezers to study membrane mechanics. Diploma thesis, Technische Universität Dresden.

39. Fantana HA (2011) Mechanics of spindle centering in Caenorhabditis elegans. PhD thesis, Technische Universität Dresden.

Supplementary Information

Movie S1. Video of a microsphere, coated with anti-tubulin antibodies that was bound specifically to a microtubule which was partly immobilized on the sample surface. This microtubule was chosen to exclude any non-specific binding between the microsphere and the surface. Scale bar: 3 µm. 2 × real-time.

Supplementary information of this article can be found online at http://www.jbmethods.org/jbm/rt/suppFiles/79.